Toxicology and Applied Pharmacology 259 (2012) 160–168

Contents lists available at SciVerse ScienceDirect

Toxicology and Applied Pharmacology

journal homepage: www.elsevier.com/locate/ytaap

Apoptosis induction by silica nanoparticles mediated through reactive oxygen species in human liver cell line HepG2

Javed Ahmad [a], Maqusood Ahamed [b,*], Mohd Javed Akhtar [c], Salman A. Alrokayan [b], Maqsood A. Siddiqui [a], Javed Musarrat [a], Abdulaziz A. Al-Khedhairy [a]

[a] Department of Zoology, College of Science, King Saud University, Riyadh 11451, Saudi Arabia
[b] King Abdullah Institute for Nanotechnology, King Saud University, Riyadh 11451, Saudi Arabia
[c] Fibre Toxicology, CSIR-Indian Institute of Toxicology Research, Lucknow-226001, India

ARTICLE INFO

Article history:
Received 1 October 2011
Revised 21 December 2011
Accepted 23 December 2011
Available online 8 January 2012

Keywords:
Silica nanoparticles
Liver toxicity
HepG2 cells
ROS
p53
Apoptosis

ABSTRACT

Silica nanoparticles are increasingly utilized in various applications including agriculture and medicine. *In vivo* studies have shown that liver is one of the primary target organ of silica nanoparticles. However, possible mechanisms of hepatotoxicity caused by silica nanoparticles still remain unclear. In this study, we explored the reactive oxygen species (ROS) mediated apoptosis induced by well-characterized 14 nm silica nanoparticles in human liver cell line HepG2. Silica nanoparticles (25–200 μg/ml) induced a dose-dependent cytotoxicity in HepG2 cells. Silica nanoparticles were also found to induce oxidative stress in dose-dependent manner indicated by induction of ROS and lipid peroxidation and depletion of glutathione (GSH). Quantitative real-time PCR and immunoblotting results showed that both the mRNA and protein expressions of cell cycle checkpoint gene p53 and apoptotic genes (bax and caspase-3) were up-regulated while the anti-apoptotic gene bcl-2 was down-regulated in silica nanoparticles treated cells. Moreover, co-treatment of ROS scavenger vitamin C significantly attenuated the modulation of apoptotic markers along with the preservation of cell viability caused by silica nanoparticles. Our data demonstrated that silica nanoparticles induced apoptosis in human liver cells, which is ROS mediated and regulated through p53, bax/bcl-2 and caspase pathways. This study suggests that toxicity mechanisms of silica nanoparticles should be further investigated at *in vivo* level.

Introduction

Silica nanoparticles are increasingly used in various applications including chemical industry, cosmetic and medicine (Bottini et al., 2007; Slowing et al., 2008; Zhu et al., 2010). The wide-spread applications of silica nanoparticles, however, increase the environmental and human exposure concern and thus the potential risk related to their short- and long-term toxicity. There are studies reported the toxicity of silica nanoparticles to bacteria (*Bacillus subtilis* and *Escherichia coli*), green algae (*Pseudokirchneriella subcapitata*) and zebrafish (*Danio rerio*) (Adams et al., 2006; Fent et al., 2010; Hoecke et al., 2008).

Silica nanoparticles can enter human body via different routes such as inhalation, ingestion, dermal contact and injection (Lam et al., 2004; Oberdoerster et al., 2005; Warheit et al., 2004; Zhou and Yokel, 2005). Silica nanoparticles injected to mice could distribute nearly in all organs and mainly accumulate, retain and induce toxic effects in lung, liver and spleen (Kaewamatawong et al., 2006; Liu et al., 2011; Park and Park, 2009). Investigators also observed that liver was one of the most target organs for silica nanoparticles (Lu et al., 2011; Nishimori et al., 2009; Xie et al., 2010). There are few important studies evaluating the toxicity of silica nanoparticles in cultured human liver cells (Li et al., 2011; Ye et al., 2010). However, possible mechanisms of hepatotoxicity due to silica nanoparticles exposure still remain unclear.

Apoptosis is induced by extracellular or intracellular signals, which trigger onset of signaling cascade with characteristic biochemical and cytological signatures including nuclear condensation and DNA fragmentation (Gopinath et al., 2010). There are several genes known to involve in apoptotic pathways. The p53 gene is able to activate cell cycle checkpoints, DNA repair and apoptosis to maintain genomic stability (Sherr, 2004). The ratio of bax/bcl-2 proteins represent a cell death switch, which determines the life or death of cells in response to an apoptotic stimulus; an increased bax/bcl-2 ratio decreases the cellular resistance to apoptotic stimuli, leading to apoptosis (Chougule et al., 2011; Gao and Wang, 2009). Also destabilization of the mitochondrial integrity by apoptotic stimuli precedes activation of caspases leading to apoptosis (Timmer and Salvesen, 2007; Youle and Strasser, 2008).

The potential mechanisms of nanoparticles toxicity are not fully explored. One mechanism often discussed is the induction of

* Corresponding author at: King Abdullah Institute for Nanotechnology, King Saud University, P.O. Box 2454, Riyadh 11451, Saudi Arabia. Fax: +966 4670664.
E-mail addresses: maqusood@gmail.com, mahamed@ksu.edu.sa (M. Ahamed).

0041-008X/$ – see front matter © 2012 Elsevier Inc. All rights reserved.
doi:10.1016/j.taap.2011.12.020

oxidative damage of cellular constituents due to the generation of reactive oxygen species (ROS) (Nel et al., 2006). Studies demonstrated that nanoparticles have potential to induce ROS mediated DNA damage and apoptosis (Ahamed et al., 2011a; Asharani et al., 2009; Park and Park, 2009). In the present study, we investigated the cytotoxicity, ROS generation and oxidative stress induced by well-characterized 14 nm amorphous silica nanoparticles in human liver cell line HepG2. Apoptosis induction by silica nanoparticles was explored via p53, bax/bcl-2, and caspase-3 pathways. We further examined the role of ROS in silica nanoparticles induced apoptosis using vitamin C, a potent ROS scavenger. This study provides molecular evidence for the ROS mediated apoptosis in human liver cells due to silica nanoparticles exposure.

Materials and methods

Silica nanoparticles and chemicals. Silica (SiO_x) nanopowder (Product No. 4850MR, Average particle size: 15 nm, specific surface area: 640 m^2/g, Purity: 99.5% trace metals basis) purchased from Nanostructured & Amorphous Materials, Inc. (Houston, TX).

Fetal bovine serum (FBS), penicillin-streptomycin and DMEM/F-12 medium were obtained from Invitrogen Co. (Carlsbad, CA). MTT [3-(4, 5-dimethylthiazol-2-yl)-2, 5-diphenyltetrazoliumbromide], 5,5-dithiobis-(2-nitrobenzoic acid) (DTNB), reduced glutathione (GSH), anti-p53 antibody, anti-bax antibody, anti-bcl-2 antibody and anti-β-actin antibody were purchased from Sigma-Aldrich (St. Louis, MO). Secondary antibodies, RIPA buffer and sodium dodecyl sulphate (SDS) were bought from Santa Cruz Biotechnology, Inc. (Santa Cruz, CA). All other chemicals used were of the highest purity available from commercial sources.

Characterization of silica nanoparticles. The amorphous nature of silica nanopowder was determined by X-ray diffraction (XRD) at room temperature with the help of PANalytical X'Pert X-ray diffractometer equipped with a Ni filtered using Cu K_α ($\lambda = 1.54056$ Å) radiations as X-ray source. Morphology and size of silica nanoparticles were evaluated by field emission scanning electron microscope (FESEM, JSM-7600 F, JEOL Inc.) and field emission transmission electron microscopy (FETEM, JEM-2100 F, JEOL Inc.) at an accelerating voltage of 15 kV and 200 kV respectively. Energy dispersive X-ray spectroscopy (EDS) analysis was used to see the elemental composition of silica nanoparticles.

Dynamic light scattering (DLS) for the characterization of hydrodynamic size and zeta potential of silica nanoparticles in the water and cell culture medium was performed on a Malvern Instruments Zetasizer Nano-ZS instrument as described by Murdock et al. (2008). Briefly, dry powder of silica nanoparticles was suspended in water and cell culture medium at a concentration of 200 μg/ml for 72 h. Then suspension of silica nanoparticles was sonicated using a sonicator bath at room temperature for 15 min at 40 W and performed the measurements.

Cell culture and treatment of silica nanoparticles. HepG2 cells, derived from human liver carcinoma, have widely been used in toxicological studies (Yang et al., 2011; Yuan et al., 2010). Cells were used between passages 10 and 20 and cultured in MEM medium supplemented with 10% FBS, 100 U/ml penicillin-streptomycin, 1 mM sodium pyruvate and 1.5 g/l sodium bicarbonate at 5% CO_2 and 37 °C. At 85% confluence, cells were harvested using 0.25% trypsin and were subcultured into 75 cm^2 flask, 6-well plate or 96-well plate according to selection of experiments. Cells were allowed to attach the surface for 24 h prior to nanoparticles exposure. Silica nanoparticles were suspended in cell culture medium and diluted to appropriate concentrations. The dilutions of silica nanoparticles were then sonicated using a sonicator bath at room temperature for 10 min at 40 W to avoid nanoparticles agglomeration prior to administration to the cells.

MTT assay. The viability of HepG2 cells after exposure to silica nanoparticles was assessed by MTT assay as described by Mossman (1983) with some modifications (Ahamed, 2011a). The MTT assay assesses the mitochondrial function by measuring ability of viable cells to reduce MTT into blue formazon product. In brief, 1×10^4 cells/well were seeded in 96-well plates and exposed to silica nanoparticles at the concentrations of 0, 1, 5, 10, 25, 50, 100 and 200 μg/ml for 72 h. After the exposure completed, the medium was removed from each well to avoid interference of nanoparticles and replaced with new medium containing MTT solution in an amount equal to 10% of culture volume, and incubated for 3 h at 37 °C until a purple colored formazan product developed. The resulting formazan product was dissolved in acidified isopropanol. Further, the 96-well plate was centrifuged at 2500 rpm for 5 min to settle down the remaining nanoparticles present in the solution. Then, a 100 μl supernatant was transferred to other fresh wells of 96-well plate and absorbance was measured at 570 by using a microplate reader (Synergy-HT, BioTek).

NRU assay. Neutral red uptake (NRU) assay was performed following the procedure as described by Borenfreund and Puerner (1984) with some modifications (Ahamed, 2011a). In brief, 1×10^4 cells/well were seeded in 96-well plates and exposed to silica nanoparticles at the concentrations of 0, 1, 5, 10, 25, 50, 100 and 200 μg/ml for 72 h. At the end of exposure the test solution was aspirated and cells were washed with PBS twice and incubated for 3 h in medium supplemented with neutral red (50 μg/ml). The medium was washed off rapidly with a solution containing 0.5% formaldehyde and 1% calcium chloride. Cells were further incubated for 20 min at 37 °C in a mixture of acetic acid (1%) and ethanol (50%) to extract the dye. Further, 96-well plate was centrifuged at 2500 rpm for 5 min to settle down the remaining nanoparticles present in the solution. Then, a 100 μl supernatant was transferred to other fresh wells of 96-well plate and absorbance was measured at 540 nm by using a microplate reader (Synergy-HT, BioTek).

Preparation of crude cell extract. For the measurement of LPO, GSH and caspase-3 enzyme, HepG2 cells were cultured in 75-cm^2 culture flask and exposed to different concentrations of silica nanoparticles (1–200 μg/ml) for 72 h. After the treatment, cells were harvested in ice-cold phosphate buffer saline by scraping and washed with phosphate buffer saline at 4 °C. The cell pellets were then lysed in cell lysis buffer [1× 20 mM Tris–HCl (pH 7.5), 150 mM NaCl, 1 mM Na_2EDTA, 1% Triton, 2.5 mM sodium pyrophosphate]. Following centrifugation (15000x g for 10 min at 4 °C) the supernatant (cell extract) was maintained on ice.

Membrane lipid peroxidation. The extent of membrane LPO was estimated by measuring the formation of malondialdehyde (MDA) using the method of Ohkawa et al. (1979). MDA is one of the end products of membrane LPO. Briefly, a mixture of 0.1 ml cell extract and 1.9 ml of 0.1 M sodium phosphate buffer (pH 7.4) was incubated at 37 °C for 1 h. After the incubation mixture was precipitated with 5% TCA and centrifuged (2300x g for 15 min at room temperature) to collect supernatant. Then 1.0 ml of 1% TBA was added to the supernatant and placed in the boiling water for 15 min. After cooling to room temperature absorbance of the mixture was taken at 532 nm and was converted to MDA and expressed in nmole MDA/mg protein using molar extinction coefficient of 1.56×10^5 M^{-1} cm^{-1}. A reaction mixture devoid of cell extract served as control.

Intracellular glutathione. GSH level was quantified using Ellman's method (1959). Briefly, a mixture of 0.1 ml of cell extract and 0.9 ml of 5% TCA was centrifuged (2300 x g for 15 min at 4 °C). Then 0.5 ml of supernatant added into 1.5 ml of 0.01% DTNB and the

reaction was monitored at 412 nm. The amount of GSH was expressed in terms of nmole/mg protein.

Measurement of reactive oxygen species. ROS were determined in HepG2 cells exposed to 200 μg/ml silica nanoparticles for 72 h. Vitamin C (1.5 mM) was also co-exposed with silica nanoparticles to delineate the role of ROS in silica nanoparticle-induced toxicity. The concentration of vitamin C used in this study was according to our previous investigations (Ahamed et al., 2011a; Akhtar et al., 2010a).

The production of intracellular ROS was measured using 2,7-dichlorofluorescin diacetate (DCFH-DA) (Wang and Joseph, 1999). The DCFH-DA passively enters the cell where it reacts with ROS to form the highly fluorescent compound dichlorofluorescein (DCF). Briefly, 10 mM DCFH-DA stock solution (in methanol) was diluted in culture medium without serum or other additive to yield a 100 μM working solution. At the end of exposure with nanoparticles and vitamin C cells were washed twice with HBSS. Then cells were incubated in 1 ml working solution of DCFH-DA at 37 °C for 30 min. Cells were lysed in alkaline solution and centrifuged at 2300 x g. A 200 μl supernatant was transferred to 96-well plate and fluorescence was measured using at 485 nm excitation and 520 nm emission using a microplate reader (Synergy-HT, BioTek). The values were expressed as percent of fluorescence intensity relative to control wells.

Total RNA isolation and quantitative real-time PCR analysis for apoptotic markers. Cells were cultured in 6-well plates and exposed to silica nanoparticles (200 μg/ml) with or without vitamin C (1.5 mM) for 72 h. At the end of exposure, total RNA was extracted by RNeasy mini Kit (Qiagen) according to the manufacturer's instructions. Concentration of the extracted RNA were determined using Nanodrop 8000 spectrophotometer (Thermo-Scientific) and the integrity of RNA were visualized on 1% agarose gel using gel documentation system (Universal Hood II, BioRad). The first strand cDNA was synthesized from 1 μg of total RNA by Reverse Transcriptase using M-MLV (Promega) and oligo (dT) primers (Promega) according to the manufacturer's protocol. Quantitative real-time PCR (RT-PCR^{q}) was performed by QuantiTect SYBR Green PCR kit (Qiagen) using ABI PRISM 7900HT Sequence Detection System (Applied Biosystems, USA). Two microliter of template cDNA was added to the final volume of 20 μl of reaction mixture. Real-time PCR cycle parameters included 10 min at 95 °C followed by 40 cycles involving denaturation at 95 °C for 15 s, annealing at 60 °C for 20s and elongation at 72 °C for 20s. The sequences of the specific sets of primer for p53, bax, bcl-2, caspase-3 and β-actin used in this study are given in our previous publication (Ahamed et al., 2011a). Expressions of selected genes were normalized to β-actin gene, which was used as an internal housekeeping control. All the real-time PCR experiments were

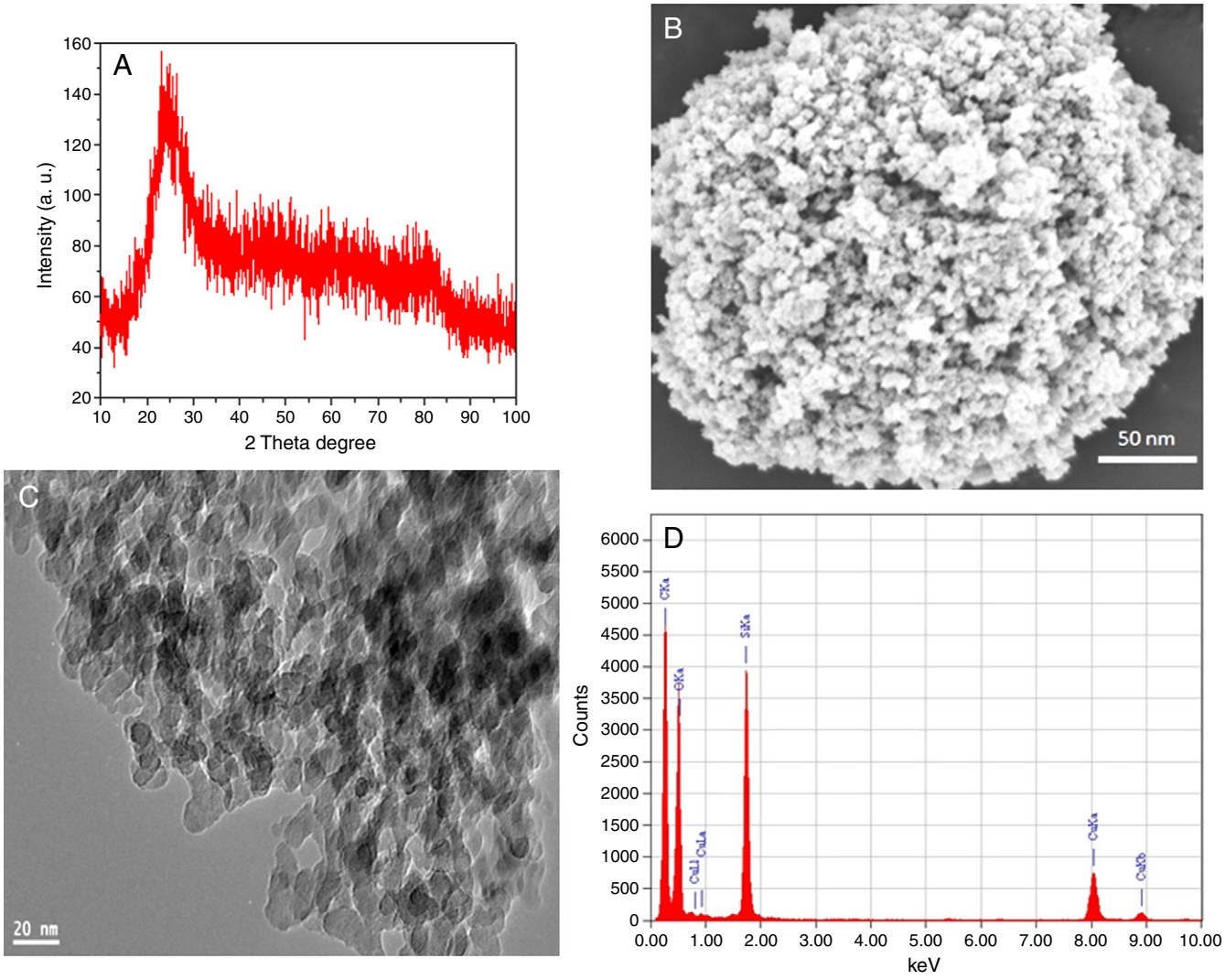

Fig. 1. Characterization of silica nanoparticles. (A) X-ray diffraction pattern of silica nanoparticles, (B) Field emission scanning electron microscope image, (C) Field emission transmission electron microscope image and (C) Energy dispersive X-ray spectrum.

Table 1
Dynamic light scattering (DLS) measurements of silica nanoparticles.

DLS measurements of silica nanoparticles		
	Water	Culture media
Hydrodynamic size (nm)	128	96
Zeta potential (−mV)	25	28

performed in triplicate and data expressed as the mean of at least three independent experiments.

Western blot analysis of apoptotic markers. Cells were cultured in 6-well plates and exposed to silica nanoparticles (200 μg/ml) with or without vitamin C (1.5 mM) for 72 h. The harvested cell pellets were lysed in RIPA lysis buffer [1x TBS (0.5 M Tris–HCl and 1.5 M NaCl) pH 7.4, 1% NP-40, 0.5% sodium deoxycholate, 0.1% SDS, 0.004% sodium azide] in the presence of protease inhibitors. The cell lysates were then analyzed for protein content using SDS-PAGE immunoblotting. The membrane was then probed with antibodies to determine levels of protein expression.

Caspase-3 enzyme assay. Activity of caspase-3 enzyme was measured in exposed and control cells using standard assay kit (BioVision, Inc.). Crude cell extract was prepared as described above. This assay is based on the principle that activated caspases in apoptotic cells cleave the synthetic substrates to release free chromophore p-nitroanilide (pNA), which is measured at 405 nm. The pNA was generated after specific action of caspase-3 on tertrapeptide substrates DEVD-pNA (Ahamed et al., 2010a; Berasain et al., 2005). The reaction mixture consisted of 50 μl of cell extract protein (50 μg), 50 μl of 2 x reaction buffer (containing 10 mM dithiothreitol) and 5 μl of 4 mM DEVD-pNA substrate in a total volume of 105 μl. The reaction mixture was incubated at 37 °C for 1 h and absorbance of the product was measured using microplate reader (Synergy-HT, BioTek) at 405 nm according to manufacturer's instruction.

Protein estimation. The total protein content in cell extracts was estimated by the Bradford method (Bradford, 1976) using bovine serum albumin as the standard.

Statistical analysis. All the data represented in this study are means ± SD of three identical experiments made in three replicate. Statistical significance was determined by one-way analysis of variance (ANOVA) followed by Dunnett's multiple comparison test. Significance was ascribed at $p<0.05$. All analyses were conducted using the Prism software package (GraphPad Software).

Results

Silica nanoparticles characterization

X-ray diffraction (XRD) analysis exhibits the amorphous nature of silica nanoparticles (Fig. 1A). Fig. 1B and C depicts the typical SEM and TEM images of silica nanoparticles respectively. TEM average diameter was calculated from measuring over 100 particles in random fields of TEM view. The average TEM diameter of silica nanoparticles was 14.23 ± 2.16 nm. The EDS spectrum of silica nanoparticles is given in Fig. 1D. The presence of Cu and C signals was from the carbon-coated Cu grid. The EDS result showing that there is no other elemental impurities present in silica nanoparticles.

The average hydrodynamic size of silica nanoparticles in water and cell culture medium was 128 and 96 nm respectively. Further, zeta-potential of silica nanoparticles in water and culture media was −25 mV and −28 mV respectively (Table 1).

Cytotoxicity induced by silica nanoparticles

HepG2 cells were exposed to silica nanoparticles at the concentrations of 0, 1, 5, 10, 25, 50, 100 and 200 μg/ml for 72 h and cytotoxicity was determined by MTT and NRU assays. Both the assays have shown that silica nanoparticles up to the concentration of 10 μg/ml did not produce significant cytotoxicity to cells ($p>0.05$ for each). As the concentration of nanoparticles increased to 25–200 μg/ml cytotoxicity was observed in a dose-dependent manner. In MTT assay, cell viability was significantly decreased to 79, 71, 64 and 55% for the concentrations of 25, 50, 100 and 200 μg/ml respectively ($p<0.05$ for each) (Fig. 2A). Fig. 2B shows the results of cell viability obtained by NRU assay. In this assay, cell viability decreased to 78, 71, 64 and 58% when cells exposed to silica nanoparticles at the concentrations of 25, 50, 100 and 200 μg/ml respectively ($p<0.05$ for each).

Oxidative stress induced by silica nanoparticles

We studied the membrane LPO and intracellular GSH levels in HepG2 cells at the concentrations of 0, 1, 5, 10, 25, 50, 100 and 200 μg/ml for 72 h. MDA level, an end product of membrane LPO was significantly higher in cells exposed to silica nanoparticles in the concentration range of 25–100 μg/ml ($p<0.05$ for each) (Fig. 3A). Fig. 3B shows that silica nanoparticles significantly reduced

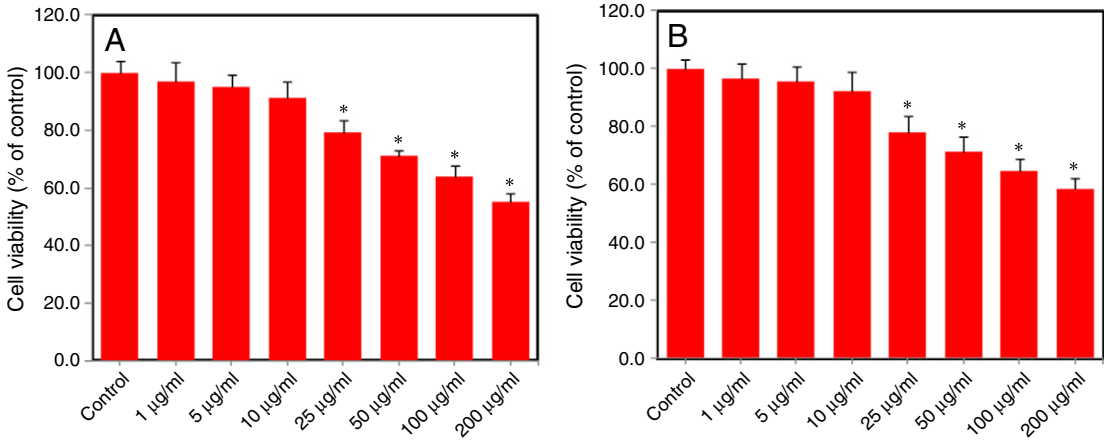

Fig. 2. Silica nanoparticle-induced cytotoxicity in HepG2 cells. Cells were treated with silica nanoparticles at the concentrations of 0, 1, 5, 10, 25, 50, 100 and 200 μg/ml for 72 h. At the end of treatment cytotoxicity parameters were determined as described in the materials and methods. (A) MTT assay and (B) NRU assay. Data represented are mean ± SD of three identical experiments made in three replicate. *Statistically significant difference as compared to the controls ($p<0.05$ for each).

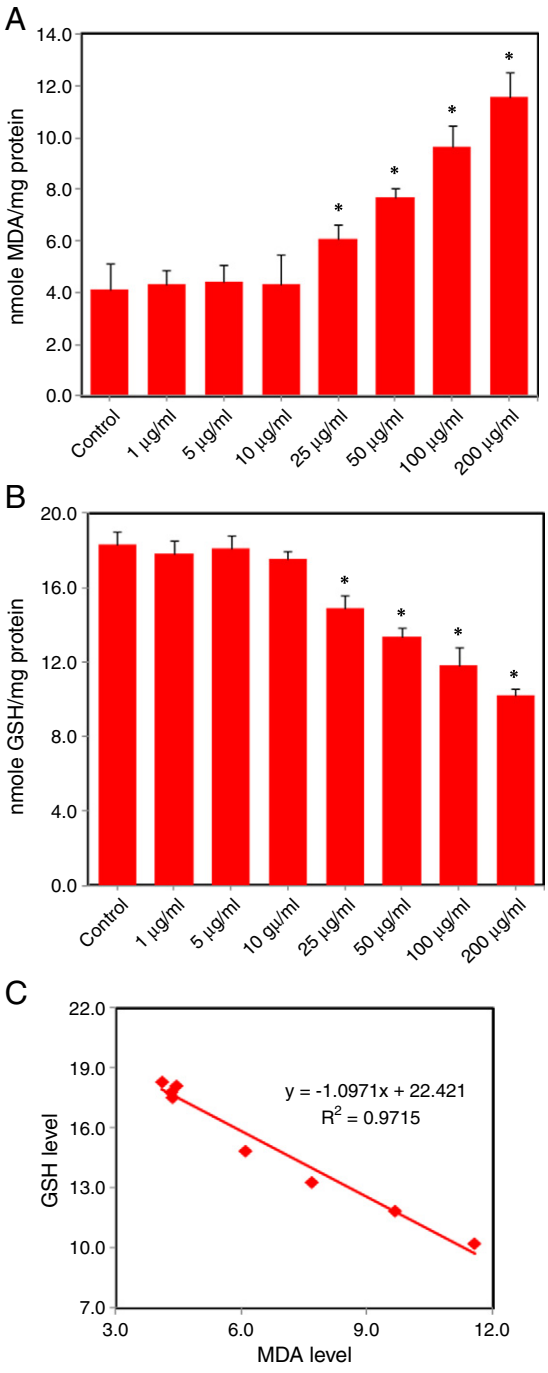

Fig. 3. Silica nanoparticle-induced oxidative stress markers in HepG2 cells. Cells were with silica nanoparticles at the concentrations of 0, 1, 5, 10, 25, 50, 100 and 200 µg/ml for 72 h. At the end of treatment MDA and GSH levels were determined as described in the materials and methods. (A) MDA level, (B) GSH level and (C) Significant negative correlation between the MDA and GSH. Data represented are mean ± SD of three identical experiments made in three replicate. *Statistically significant difference as compared to the controls ($p<0.05$ for each).

the intracellular level of GSH in a dose-dependent manner ($p<0.05$ for each). Further, we found a significant negative correlation between oxidant (MDA) generation and antioxidant (GSH) depletion in HepG2 cells exposed silica nanoparticles (Fig. 3C). Significant negative correlation between oxidant (MDA) production and cell viability (MTT) reduction was also observed (Fig. 4).

We further examined the effect of 200 µg/ml silica nanoparticles on the generation of ROS in the presence or absence of vitamin C. Fig. 5

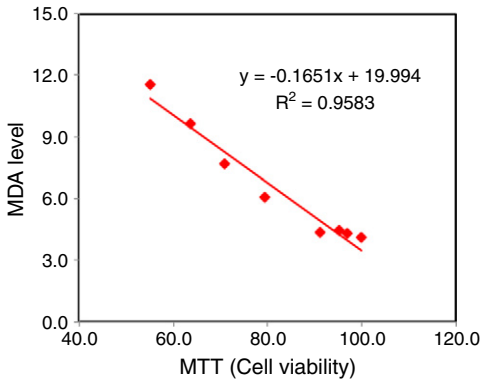

Fig. 4. Significant negative correlation between oxidant (MDA) and reduction in cell viability (MTT) in HepG2 cells exposed to silica nanoparticles.

shows that the silica nanoparticles significantly induced the intracellular production of ROS ($p<0.05$). We also noted that co-exposure of vitamin C effectively prevented the ROS generation induced by silica nanoparticles. ROS level was reduced up to control level for silica nanoparticles in the presence of ascorbic acid (Fig. 5). When the silica nanoparticles induced ROS was 1.56 fold, in the presence of vitamin C it was reduced and found to be 1.14 fold of control level.

Reactive oxygen species mediated alterations in the expression of mRNA of apoptotic genes by silica nanoparticles

We utilized quantitative real-time PCR to analyze the mRNA levels of apoptotic genes (p53, bax, bcl-2 and caspase-3) in HepG2 cells exposed silica nanoparticles in the presence or absence of vitamin C. Results showed that silica nanoparticles significantly altered the expression levels of mRNA of these genes in HepG2 cells. The mRNA expression levels of cell cycle checkpoint gene p53 (Fig. 6A) and pro-apoptotic gene bax (Fig. 6B) were up-regulated while the expression of anti-apoptotic gene bcl-2 (Fig. 6C) was down-regulated in treated cells. We also observed the higher expression of caspase-3 gene in treated cells than those of the controls (Fig. 6D). Furthermore, we observed that silica nanoparticles induced alterations in apoptotic genes were significantly attenuated by vitamin C, a potent ROS scavenger.

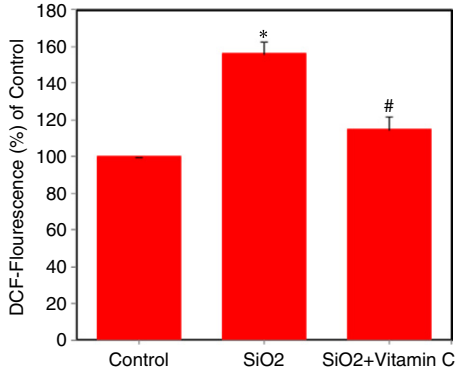

Fig. 5. Silica nanoparticle-induced reactive oxygen species generation in HepG2 cells. Cells were treated with silica nanoparticles (200 µg/ml) in the presence or absence of vitamin C (1.5 mM) for 72 h. At the end of treatment ROS levels were determined as described in materials and methods. Data represented are mean ± SD of three identical experiments made in three replicate. *Statistically significant difference in ROS generation as compared to the controls ($p<0.05$). #Significant inhibitory effect of vitamin C on ROS generation ($p<0.05$).

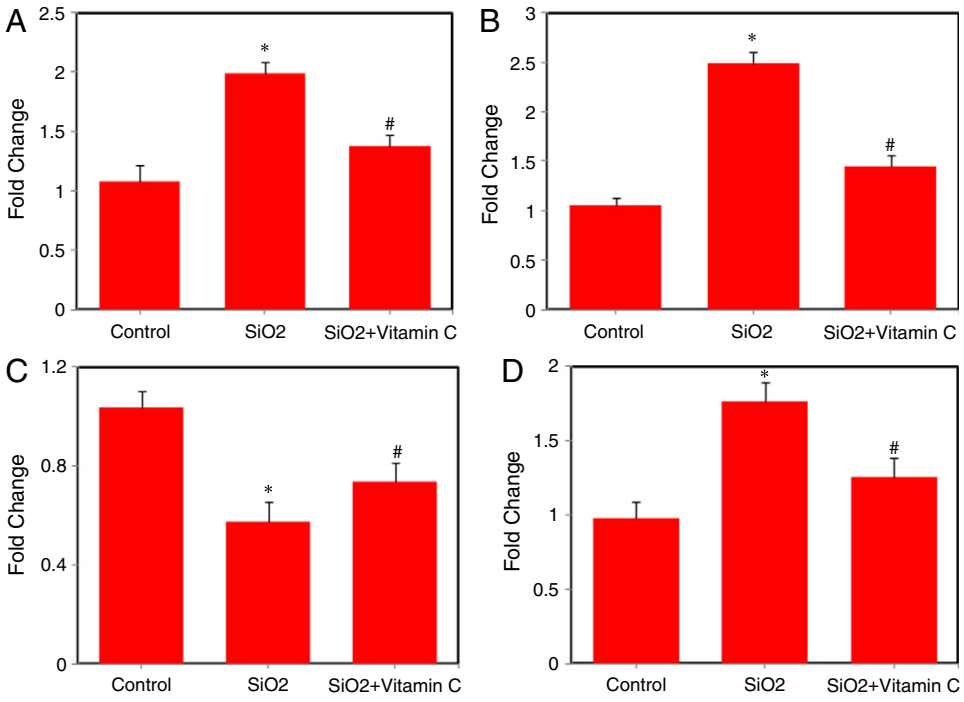

Fig. 6. Quantitative real-time PCR analysis of mRNA levels of apoptotic genes in HepG2 cells due to silica nanoparticles exposure. Cells were treated with silica nanoparticles (200 μg/ml) in the presence or absence of vitamin C (1.5 mM) for 72 h. Quantitative real-time PCR (RT-PCR[q]) was performed by QuantiTect SYBR Green PCR kit using ABI PRISM 7900HT Sequence Detection System. The β-actin was used as the internal control to normalize the data. Silica nanopaticle-induced alterations in mRNA expression levels are expressed in relative quantity compared with those for the respective unexposed control cells. Data represented are mean ± SD of three identical experiments made in three replicate. *Statistically significant difference as compared to the controls ($p<0.05$ for each). #Significant inhibitory effect of vitamin C on m RNA expressions of genotoxic markers ($p<0.05$ for each).

Reactive oxygen species mediated alterations in the expression of proteins of apoptotic genes by silica nanoparticles

To verify mRNA results, we further examined the expression of apoptotic genes at protein levels in nanoparticles exposed HepG2 cells using immunobloting. Like real-time PCR results the protein level of p53 and bax were significantly up-regulated while the expression of bcl-2 was significantly down-regulated in silica nanoparticles treated cells. Silica nanoparticles induced alterations in the apoptotic proteins were also significantly prevented by ROS scavenger vitamin C (Fig. 7A and B).

Moreover, we found that co-exposure of vitamin C effectively reduced the activity of caspase-3 enzyme induced by silica nanoparticles. When the silica nanoparticles induced caspase-3 activity was 1.87 fold, in the presence of vitamin C it was reduced and found to be 1.28 fold of control level (Fig. 7C).

Vitamin C prevented the reduction of cell viability caused by silica nanoparticles

The potential of vitamin C to prevent the reduction of cell viability caused by silica nanoparticles in HepG2 cells was examined by MTT assay. Cells were exposed to silica nanoparticles at the concentration of 200 μg/ml for 72 h in the presence or absence of vitamin C. We observed that co-exposure of vitamin C significantly prevented the cell viability reduction induced by silica nanoparticles. Cell viability reduction due to silica nanoparticles exposure was 55% as compared to untreated control cells, where as in the presence of vitamin C cell viability was preserved up to 90% than those of the control (Fig. 8).

Discussion

It has been suggested that the physicochemical properties of nanoparticles should be appropriately characterized before their nanotoxicity research (Balbus et al., 2007; Li et al., 2011; Murdock et al., 2008; Yu et al., 2009). We utilized XRD, SEM, TEM, EDS and DLS techniques to characterize the present silica nanoparticles. Amorphous nature of silica nanoparticles was confirmed by XRD. SEM and TEM showed that nanoparticles were almost spherical in shape, smooth surface and with an average diameter of 14 nm. EDS result indicated that present silica nanoparticles were pure with no traces of impurities. The average hydrodynamic size of silica nanoparticles in water and cell culture medium as determined by DLS was 128 and 96 nm respectively. We observed that the hydrodynamic size of silica nanoparticles measured by DLS was approximately 7–8 times higher than those calculated from TEM. The higher size of nanoparticles in aqueous suspension as compared to TEM size might be due to the tendency of particles to agglomerate in aqueous state. This finding is supported by other investigators (Bai et al., 2009) and has been briefly discussed in our previous publication (Ahamed et al., 2010a). The tendency of particles to form aggregates depends on the surface charge. The surface charge of silica nanoparitcles determined as zeta potential was −25 mV and −28 mV for water and culture medium respectively.

The potential applications of silica nanoparticles in the treatment of diseases need constant nanoparticle concentration in the blood or targeting of specific cells or organs. The suitability of silica nanoparticles in biomedical applications especially in drug delivery must be supported by rigorous studies of their potential toxicity to different organs including liver prior to full development as adjuncts to clinically useful formulations (Julien et al., 2010; Ye and Mahato, 2008). This prompted us to investigate the toxic potential of silica nanoparticles in human liver cells (HepG2). This cell line retains the functions of fully differentiated primary hepatocytes and widely used as a model system for hepatotoxicity studies (Cao et al., 2008; Zou et al., 2011). We employed two assays (MTT and NRU) to

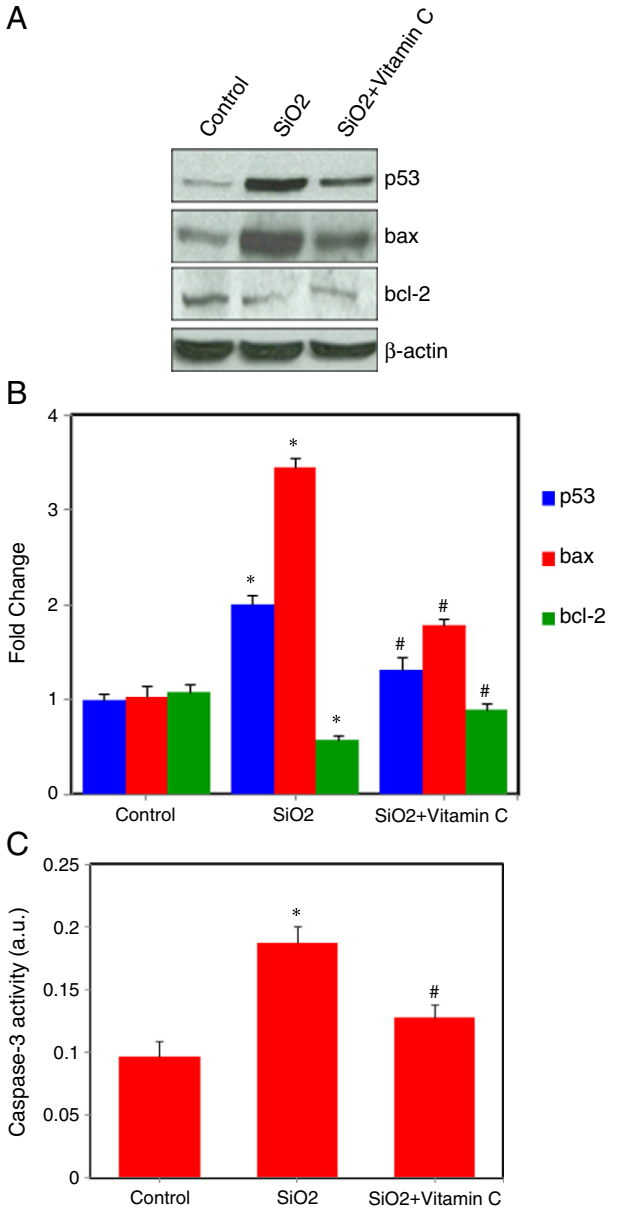

Fig. 7. Western blot analysis of protein levels of apoptotic genes in HepG2 cells due to silica nanoparticles exposure. Cells were treated with silica nanoparticles (200 μg/ml) in the presence or absence of vitamin C (1.5 mM) for 72 h. The treated and untreated cells were lysed in RIPA buffer and cell extract subjected to Western blots with anti-p53, anti-bax and anti-bcl-2 antibody as described in the materials and methods. Immunoblot images are the representative of three identical experiments. The β-actin blot is a loading control. (A) Immunoblot images of p53, bax, bcl-2 and bax proteins. (B) Protein levels were also analyzed by desitometric analysis using AlphaEase TM FC StandAlone V.4.0.0 software. Results are expressed as a fold change over the control group. (C) Silica nanoparticles induced the activity of Caspase-3 enzyme in HepG2 cells. Bar diagrams are from mean ± SD of three blots. *Statistically significant difference as compared to the controls ($p<0.05$ for each). #Significant inhibitory effect of vitamin C on protein expressions of genotoxic markers ($p<0.05$ for each).

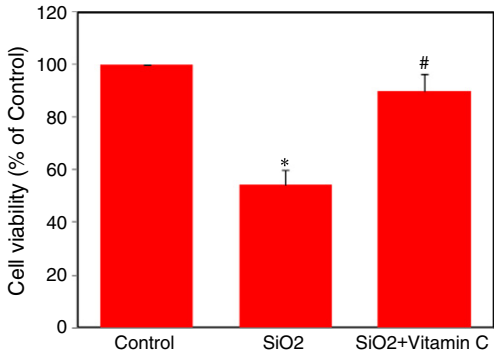

Fig. 8. Vitamin C significantly preserved the viability of HepG2 cells caused by silica nanoparticles. Cells were treated with silica nanoparticles (200 μg/ml) in the presence or absence of vitamin C (1.5 mM) for 72 h. At the end of treatment cell viability was determined using MTT assay as described in materials and methods. Data represented are mean ± SD of three identical experiments made in three replicate. *Statistically significant difference in percentage of cells as compared to the controls ($p<0.05$). #Significant inhibitory effect of vitamin C on cell viability reduction ($p<0.05$).

evaluate the cytotoxicity of silica nanoparticles to get more dependable data. In general, MTT and NRU assays are frequently utilized to determine the cytotoxicity of nanoparticles in cell culture systems (Ahamed et al., 2011a; Akhtar et al., 2010a; 2010b; Barillet et al., 2010; Mahmoudi et al., 2009). Both assays demonstrated that 14 nm silica nanoparticles produce significant cytotoxicity to HepG2 cells in dose-dependent manner in the concentration range of 25–200 μg/ml. Our cytotoxicity results are in agreement to the recent results of Li et al. (2011). They reported that 19 nm silica nanoparticles at 100 μg/ml concentration produce significant reduction in viability of human liver cells. Cytotoxicity of silica nanoparticles in different types of mammalian cells was also reported (Akhtar et al., 2010b; Julien et al., 2010; Lison et al., 2008; Wang et al., 2009).

Oxidative stress has been suggested to play an important role in the mechanisms of toxicity of a number of nanoparticles whether by the excessive generation of ROS or by depletion of cellular antioxidant capacity (Ahamed et al., 2010b; Wise et al., 2010). There has been an increase in biochemical, clinical and epidemiological evidences that indicate the involvement of ROS and oxidative stress in various diseases including cancer (Benz and Yau, 2008; Jomova and Valko, 2011). Our previous studies highlight that metal and metal oxide nanoparticles are able to induce ROS generation and oxidative stress in different types of cells (Ahamed et al., 2008; 2010a; 2010b; 2011a; 2011b). In the present study, ROS and MDA levels were significantly higher while the antioxidant GSH level was significantly lower in HepG2 cells exposed to silica nanoparticles.

ROS such as superoxide anion (O^{2-}), hydroxyl radical ($HO^{\bullet}$) and hydrogen peroxide (H_2O_2) elicit a variety of physiological and cellular events including inflammation, DNA damage and apoptosis (Ahamed et al., 2011b; Asharani et al., 2009; Nel et al., 2006). We demonstrated that the expressions of both mRNA and protein levels of cell cycle checkpoint gene p53 and pro-apoptotic genes (bax and caspase-3) were up-regulated, whereas the expression of anti-apoptotic gene bcl-2 was down-regulated in HepG2 cells due to silica nanoparticles exposure. It has been suggested that bax is up-regulated by p53 (Gopinath et al., 2010). Since an increase in bax expression was observed, the role of p53 in the up-regulation of bax upon silica nanoparticles exposure can be postulated. The insertion of bax into the mitochondrial membrane possibly leads to p53-mediated apoptosis (Gopinath et al., 2010). Caspases are activated during apoptosis in many cells and are known to play a vital role in both initiation and execution of apoptosis. It was reported that caspase-3 is essential for cellular DNA damage and apoptosis (Janicke et al., 1998). Earlier, Ye et al. (2010) reported that ROS-mediated oxidative stress, the activation of p53 and up-regulation of bax/bcl-2 ratio are involved in the silica nanoparticle-induced apoptosis in normal human liver cell line L-02. However, they did not explore the direct involvement of ROS in silica nanoparticle-induced apoptosis. Therefore, in this work we studied direct involvement of ROS in apoptosis induced by silica nanoparticles using a well known ROS scavenger vitamin C. Interestingly, co-exposure of vitamin C significantly ameliorated the modulations of apoptotic genes both at mRNA and protein levels caused by silica nanoparticles. We provide the evidence that silica

nanoparticles induced apoptosis mediated through ROS via p53, bax/bcl-2 and caspase pathways in HepG2 cells. We also showed that vitamin C preserved the reduction in cell viability caused by silica nanoparticles. This study is supported by our previous publications where quantitative real-time PCR and Western blot analysis demonstrated that nanoparticles significantly up-regulated the expression p53, bax and caspases, and down-regulated bcl-2 in cultured human cells (Ahamed et al., 2008, 2010c, 2011a, 2011b).

As with most published work in nanotoxicology, the high concentration-induced toxicity observed in this study may be difficult to translate to a realistic human exposure. We believe these data are positioned to provide a springboard for other researchers to create mechanistic pathways in-depth involved in silica nanoparticles induced toxicity and provide knowledge for this important deficiency in this rapidly evolving area of human exposure concern (Hussain and Schlager, 2009; Sung et al., 2009).

In conclusion, silica nanoparticles induced cytotoxicity and oxidative stress in human liver (HepG2) cells in a dose-dependent manner. Both the mRNA and protein expressions of cell cycle check point gene p53 and apoptotic genes (bax and caspase-3) were up-regulated while the anti-apotoic gene bcl-2 was down-regulated in cells treated with silica nanoparticles. Moreover, co-treatment of ROS scavenger vitamin C significantly attenuated the alteration of apoptotic markers along with the preservation of cell viability caused by silica nanoparticles. This study suggests that the application of silica nanoparticles should be carefully evaluated as to their potential toxic effect to human health.

Conflict of interest statement

The authors declare that there are no conflicts of interest.

Acknowledgments

This work was supported by King Abdulaziz City for Science and Technology (KACST) under the National Plan for Science and Technology (NPST) (Grant No.: 10-NAN1201-02).

References

Adams, L.K., Lyon, D.Y., Alvarez, P.J., 2006. Comparative eco-toxicity of nanoscale TiO2, SiO2, and ZnO water suspensions. Water Res. 40, 3527–3532.
Ahamed, M., 2011. Toxic response of nickel nanoparticles in human lung epithelial A549 cells. Toxicol. in Vitro 25, 930–936.
Ahamed, M., Karns, M., Goodson, M., Rowe, J., Hussain, S., Schlager, J., Hong, Y., 2008. DNA damage response to different surface chemistry of silver nanoparticles in mammalian cells. Toxicol. Appl. Pharmacol. 233, 404–410.
Ahamed, M., Posgai, R., Gorey, T.J., Nielsen, M., Hussain, S., Rowe, J., 2010a. Silver nanoparticles induced heat shock protein 70, oxidative stress and apoptosis in Drosophila melanogaster. Toxicol. Appl. Pharmacol. 242, 263–269.
Ahamed, M., AlSalhi, M.S., Siddiqui, M.K.J., 2010b. Silver nanoparticle applications and human health. Clin. Chim. Acta 411, 1841–1848.
Ahamed, M., Siddiqui, M.A., Akhtar, M.J., Ahmad, I., Pant, A.B., Alhadlaq, H.A., 2010c. Genotoxic potential of copper oxide nanoparticles in human lung epithelial cells. Biochem. Biophys. Res. Commun. 396, 578–583.
Ahamed, M., Akhtar, M.J., Siddiqui, M.A., Ahmad, J., Musarrat, J., Al-Khedhairy, A.A., AlSalhi, M.S., Alrokayan, S.A., 2011a. Oxidative stress mediated apoptosis induced by nickel ferrite nanoparticles in cultured A549 cells. Toxicology 283, 101–108.
Ahamed, M., Akhtar, M.J., Raja, M., Ahmad, I., Siddiqui, M.K.J., AlSalhi, M.S., Alrokayan, S.A., 2011b. ZnO nanorod-induced apoptosis in human alveolar adenocarcinoma cells via p53, survivin and bax/bcl-2 pathways: Role of oxidative stress. Nanomedicine NBM 7, 904–913.
Akhtar, M.J., Kumar, S., Murthy, R.C., Ashquin, M., Khan, M.I., Patil, G., Ahmad, I., 2010a. The primary role of iron-mediated lipid peroxidation in the differential cytotoxicity caused by two varieties of talc nanoparticles on A549 cells and lipid peroxidation inhibitory effect exerted by ascorbic acid. Toxicol. In Vitro 24, 1139–1147.
Akhtar, M.J., Ahamed, M., Kumar, S., Siddiqui, H., Patil, G., Ashquin, M., Ahmad, I., 2010b. Nanotoxicity of pure silica mediated through oxidant generation rather than glutathione depletion in human lung epithelial cells. Toxicology 276, 95–102.
Asharani, P.V., Mun, G.K., Hande, M.P., Valiyaveettil, S., 2009. Cytotoxicity and genotoxicity of silver nanoparticles in human cells. ACS Nano 3, 279–290.
Bai, W., Zhang, Z., Tian, W., He, X., Ma, Y., Zhao, Y., Chai, Z., 2009. Toxicity of zinc oxide nanoparticles to zebrafish embryo: a physicochemical study of toxicity mechanism. J. Nanopart. Res. 12, 1645–1654.
Balbus, J.M., Maynard, A.D., Colvin, V.L., Castranova, V., Daston, G.P., Denison, R.A., 2007. Meeting report: hazard assessment for nanoparticles-report from an interdisciplinary workshop. Environ. Health Perspect. 115, 1654–1659.
Barillet, S., Jugan, M.L., Laye, M., Leconte, Y., Herlin-Boime, N., Reynaud, C., Carriere, M., 2010. In vitro evaluation of SiC nanoparticles impact on A549 pulmonary cells: cyto-, genotoxicity and oxidative stress. Toxicol. Lett. 198, 324–330.
Benz, C.C., Yau, C., 2008. Ageing, oxidative stress and cancer: paradigms in parallax. Nat. Rev. Cancer 8, 875–879.
Berasain, C., Garcia-Trevijano, E.R., Castillo, J., Erroba, E., Santamaria, M., Lee, D.C., 2005. Novel role for amphiregulin in protection from liver injury. J. Biol. Chem. 280, 19012–19020.
Borenfreund, E., Puerner, J.A., 1984. A simple quantitative procedure using monolayer cultures for cytotoxicity assays. J. Tissue Cult. Method 9, 7–9.
Bottini, M., D'Annibale, F., Magrini, A., Cerignoli, F., Arimura, Y., Dawson, M.I., Bergamaschi, E., Rosato, N., Bergamaschi, A., Mustelin, T., 2007. Quantum dot-doped silica nanoparticles as probes for targeting of T-lymphocytes. Int. J. Nanomedicine 2, 227–233.
Bradford, M.M., 1976. A rapid and sensitive for the quantitation of microgram quantities of protein utilizing the principle of protein-dye binding. Anal. Biochem. 72, 248–254.
Cao, J., Liu, Y., Jia, L., Jiang, L.P., Geng, C.Y., Yao, X.F., Kong, Y., Jiang, B.N., Zhong, L.F., 2008. Curcumin attenuates acrylamide-induced cytotoxicity and genotoxicity in HepG2 cells by ROS scavenging. J. Agric. Food Chem. 56, 12059–12063.
Chougule, M., Patel, A.R., Sachdeva, P., Jackson, T., Singh, M., 2011. Anticancer activity of Noscapine, an opioid alkaloid in combination with cisplatin in human nonsmall cell lung cancer. Lung Cancer 71, 271–281.
Ellman, G.I., 1959. Tissue sulfhydryl groups. Arch. Biochem. Biophys. 82, 70–77.
Fent, K., Weisbrod, C.J., Wirth-Heller, A., Pieles, U., 2010. Assessment of uptake and toxicity of fluorescent silica nanoparticles in zebrafish (Danio rerio) early life stages. Aquat. Toxicol. 100, 218–228.
Gao, C., Wang, A.Y., 2009. Significance of increased apoptosis and bax expression in human small intestinal adenocarcinoma. J. Histochem. Cytochem. 57, 1139–1148.
Gopinath, P., Gogoi, S.K., Sanpui, P., Paul, A., Chattopadhyay, A., Ghosh, S.S., 2010. Signaling gene cascade in silver nanoparticle induced apoptosis. Colloids Surf. B 77, 240–245.
Hoecke, K.V., De Schamphelaere, K.A.C., der Meeren, P.V., Lucas, S., Janssen, C.R., 2008. Ecotoxicity of silica nanoparticles to the green alga Pseudokirchneriella subcapitata: importance of surface area. Environ. Toxicol. Chem. 27, 1948–1957.
Hussain, S.M., Schlager, J.J., 2009. Safety evaluation of silver nanoparticles: inhalation model for chronic exposure. Toxicol. Sci. 108, 223–224.
Janicke, R.U., Sprengart, M.L., Wati, M.R., Porter, A.G., 1998. Caspase-3 is required for DNA fragmentation and morphological changes associated with apoptosis. J. Biol. Chem. 273, 9357–9360.
Jomova, K., Valko, M., 2011. Advances in metal-induced oxidative stress and human disease. Toxicology 283, 65–87.
Julien, D.C., Richardson, C.C., Beaux II, M.F., McIlroy, D.N., Hill, R.A., 2010. In vitro proliferating cell models to study cytotoxicity of silica nanowires. Nanomedicine 6, 84–92.
Kaewamatawong, T., Shimada, A., Okajima, M., Inoue, H., Morita, T., Inoue, K., Takano, H., 2006. Acute and subacute pulmonary toxicity of low dose of ultrafine colloidal silica particles in mice after intratracheal instillation. Toxicol. Pathol. 34, 958–965.
Lam, C.W., James, J.T., McClustkey, R., Hunter, R., 2004. Pulmonary toxicity of single-wall carbon nanotubes in mice 7 and 90 days after intratracheal instillation. Toxicol. Sci. 77, 126–134.
Li, Y., Sun, L., Jin, M., Du, Z., Liu, X., Guo, C., et al., 2011. Size-dependent cytotoxicity of amorphous silica nanoparticles in human hepatoma HepG2 cells. Toxicol. In Vitro 25, 1343–1352.
Lison, D., Thomassen, L.C.J., Rabolli, V., Gonzalez, L., Napierska, D., Seo, J.W., et al., 2008. Nominal and effective dosimetry of silica nanoparticles in cytotoxicity assays. Toxicol. Sci. 104, 155–162.
Liu, T., Li, L., Teng, X., Huang, X., Liu, H., Chen, D., Ren, J., He, J., Tang, F., 2011. Single and repeated dose toxicity of mesoporous hollow silica nanoparticles in intravenously exposed mice. Biomaterials 32, 1657–1668.
Lu, X., Tian, Y., Zhao, Q., Jin, T., Xiao, S., Fan, X., 2011. Integrated metabonomics analysis of the size-response relationship of silica nanoparticles-induced toxicity in mice. Nanotechnology 22, 055101 (16 pp).
Mahmoudi, M., Simchi, A., Milani, A.S., Stroeve, P., 2009. Cell toxicity of superparamagnetic iron oxide nanoparticles. J. Colloid Interface Sci. 336, 510–518.
Mossman, T., 1983. Rapid colorimetric assay for cellular growth and survival: application to proliferation and cytotoxicity assays. J. Immunol. Methods 65, 55–63.
Murdock, R.C., Braydich-Stolle, L., Schrand, A.M., Schlager, J.J., Hussain, S.M., 2008. Characterization of nanomaterial dispersion in solution prior to in vitro exposure using dynamic light scattering technique. Toxicol. Sci. 101, 239–253.
Nel, A., Xia, T., Madler, L., Lin, N., 2006. Toxic potential of materials at the nano level. Science 311, 622–627.
Nishimori, H., Kondoh, M., Isoda, K., Tsunoda, S., Tsutsumi, Y., Yagi, K., 2009. Silica nanoparticles as hepatotoxicants. Eur. J. Pharm. Biopharm. 72, 496–501.
Oberdoerster, G., Oberdoerster, E., Oberdoerster, J., 2005. Nanotoxicology: an emerging discipline evolving from studies of ultrafine particles. Environ. Health Perspect. 113, 823–839.
Ohkawa, H., Ohishi, N., Yagi, K., 1979. Assay for lipid peroxides in animal tissues by thiobarbituric acid reaction. Anal. Biochem. 95, 351–358.
Park, E.J., Park, K., 2009. Oxidative stress and pro-inflammatory responses induced by silica nanoparticles in vivo and in vitro. Toxicol. Lett. 184, 18–25.
Sherr, C.J., 2004. Principles of tumor suppression. Cell 11, 235–246.

Slowing, I.I., Vivero-Escoto, J.L., Wu, C.W., Lin, V.Y., 2008. Mesoporous silica nanoparticles as controlled release drug delivery and gene transfection carriers. Adv. Drug Deliv. Rev. 60, 1278–1288.
Sung, J.H., Ji, J.H., Park, J.D., Yoon, J.U., Kim, D.S., Jeon, K.S., et al., 2009. Sub-chronic inhalation toxicity of silver nanoparticles. Toxicol. Sci. 108, 452–461.
Timmer, J.C., Salvesen, G.S., 2007. Caspase substrates. Cell Death Differ. 14, 66–72.
Wang, F., Gao, F., Lan, M., Yuan, H., Huang, Y., Liu, J., 2009. Oxidative stress contributes to silica nanoparticle-induced cytotoxicity in human embryonic kidney cells. Toxicol. In Vitro 23, 808–815.
Wang, H., Joseph, J.A., 1999. Quantifying cellular oxidative stress by dichlorofluorescein assay using microplate reader. Free Radic. Biol. Med. 27, 612–661.
Warheit, D.B., Laurence, B.R., Reed, K.L., Roach, D.H., Reynolds, G.A.M., Weff, T.R., 2004. Comparative pulmonary toxicity assessment of single-wall carbon nanotubes in rats. Toxicol. Sci. 77, 117–125.
Wise, J.P., Goodale, B.C., Wise, S.S., 2010. Silver nanospheres are cytotoxic and genotoxic to fish cells. Aquat. Toxicol. 97, 34–41.
Xie, G., Sun, J., Zhong, G., Shi, L., Zhang, D., 2010. Biodistribution and toxicity of intravenously administered silica nanoparticles in mice. Arch. Toxicol. 84, 183–190.
Yang, L., Liu, X., Lu, Z., Chan, J., Zhou, L., Fung, K.P., Wu, P., Wu, S., 2011. Ursolic acid induces doxorubicin-resistant HepG2 cell death via the release of apoptosis-inducing factor. Cancer Lett. 298, 128–138.
Ye, Z., Mahato, R.I., 2008. Role of nanomedicines in cell-based therapeutics. Nanomedicine 3, 5–8.
Ye, Y., Liu, J., Xu, J., Sun, L., Chen, M., Lan, M., 2010. Nano-SiO2 induces apoptosis via activation of p53 and Bax mediated by oxidative stress in human hepatic cell line. Toxicol. in Vitro 24, 751–758.
Youle, R.J., Strasser, A., 2008. The BCL-2 protein family: opposing activities that mediate cell death. Nat. Rev. Mol. Cell Biol. 9, 47–59.
Yu, K.O., Grabinski, C.M., Schrand, A.M., Murdock, R.C., Wang, W., Gu, B., Schlager, J.J., Hussain, S.M., 2009. Toxicity of amorphous silica nanoparticles in mouse keratinocytes. J. Nanopart. Res. 11, 15–24.
Yuan, Y., Liu, C., Qian, J., Wang, J., Zhang, Y., 2010. Size-mediated cytotoxicity and apoptosis of hydroxyapatite nanoparticles in human hepatoma HepG2 cells. Biomaterials 31, 730–740.
Zhou, Y., Yokel, R., 2005. The chemical species of aluminum influence its paracellular flux and uptake into Caco-2 cells, a model of gastrointestinal absorption. Toxicol. Sci. 87, 15–26.
Zhu, Y., Ikoma, T., Hanagata, N., Kaskel, S., 2010. Rattle-type Fe(3)O(4)@SiO(2) hollow mesoporous spheres as carriers for drug delivery. Small 6, 471–478.
Zou, J., Chen, Q., Jin, X., Tang, S., Chen, K., Zhang, T., Xia, X., 2011. Olaquindox induces apoptosis through the mitochondrial pathway in HepG2 cells. Toxicology. 285, 104–133.